JOURNAL OF APPLIED ELECTROCHEMISTRY 17 (1987) 253–260

*On the electrodeposition and characterization of niobium from fused fluoride electrolytes**

G. P. CAPSIMALIS, E. S. CHEN, R. E. PETERSON

US Army Armament, Munitions and Chemical Command Armament Research and Development Center, Large Caliber Weapon Systems Laboratory, Benet Weapons Laboratory, Watervliet, NY 12189-5000, USA

I. AHMAD

US Army Research, Development and Standardization Group, London, UK

Received 10 April 1986

The electrodeposition of niobium from a binary electrolyte consisting of KF and NaF was characterized and compared with that from the ternary electrolyte of LiF, NaF and KF. The deposition experiments were conducted at current densities between 5 and 35 mA cm^{-2} and electrolyte temperatures between 725 and 800° C. DTA measurements indicated the melting points to be 450 and 710° C for the ternary and binary electrolytes with added K_2NbF_7; however, it was necessary to operate both electrolytes above 725° C to obtain dense coherent deposits. Coating morphology was described by optical and scanning electron microscopy studies, while coating structure and properties were characterized by X-ray diffraction analysis. In particular, a series of diffraction measurements were reported to describe the changes in the microstructure of the deposited material as a function of the preparation conditions.

1. Introduction

The electrodeposition of refractory metal coatings from molten salts appears to be a promising surface-finishing method for protecting metals against corrosion and high temperature oxidation. Currently, a number of melts are available for plating a variety of metals including tantalum, niobium, molybdenum, zirconium and tungsten [1–4]. Of these metals, niobium is one of the most widely investigated [5–9], and appears to have the potential to be developed for ordnance applications. In this regard, strength, low stress and high hardness are additional properties needed to withstand both corrosion and erosion environments. In this study a comparative investigation is made of the effects of temperature, current density and additives on the electrodeposition of niobium from the fused salt systems KF–NaF and LiF–NaF–KF (FLINAK). The morphology and structure of the deposits were characterized both metallographically and by SEM and X-ray diffraction.

2. Experimental details

The solvents used consisted of (i) a binary eutectic mixture of NaF–KF, and (ii) a ternary eutectic mixture of KiF–NaF–KF prepared from reagent grade chemicals. The procedure for preparing the fused niobium electrolytes involved the addition of 3.2 wt % K_2NbF_7 to the binary eutectic, 2.5 wt % to the ternary eutectic, and outgassing the mixture under vacuum at 400° C for one week to remove adsorbed moisture. The dried mixtures were fused in nickel crucibles in an argon atmosphere. Purification consisted of prolonged electrolysis until fairly consistent cathode efficiencies were obtained. The plating of niobium alloys containing chromium or

* This paper was presented at a workshop on the electrodeposition of refractory metals, held at Imperial College, London, in July 1985.

0021–891X/87 $03.00 + .12

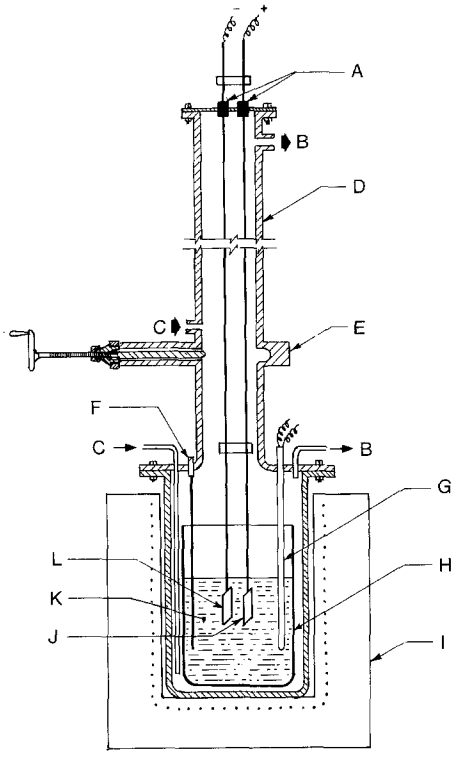

Fig. 1. Electroplating cell: A, seals; B, argon gas exit; C, argon gas entry; D, stainless steel reactor; E, gate valve; F, auxiliary electrode; G, thermocouple; H, nickel crucible; I, furnace; J, niobium anode; K, electrolyte; L, copper cathode.

boron was conducted by adding K_3CrF_6, up to 5.0 wt %, and $NaBF_4$ at 10 wt % to KF–NaF. Niobium–tantalum alloy plating was also investigated by adding up to 12.5 wt % K_2TaF_7 to FLINAK.

A diagram of the electrochemical cell used in this study is shown schematically in Fig. 1. The reactor container was constructed from 316 stainless steel and heated with a single-zone Mellor furnace. A proportional controller was used to regulate the furnace temperature. Metallurgical grade niobium and OFHC copper plates with an immersed area of 1.8 by 2.5 cm were used as electrodes. To monitor the temperature of the fused electrolyte, a platinum–platinum rhodium thermocouple housed in a closed-end nickel tube was used.

The X-ray study used an approach similar to the method of inverse pole figures to determine the texture coefficients of the deposited coatings. The calculated texture coefficients provided a good representation of the fibre texture normal to the deposition plane of the sample. A Philips X-ray diffractometer was employed to scan each sample for the various X-ray intensity peaks in the 2θ range of 0 to 76.00°. MoK_α radiation (λ = 0.70926 A) was monochromatized by means of an LiF curved crystal. The X-ray generator was operated at 45 kV and 15 mA. A one-degree divergence of the incident beam was maintained by a 2θ compensating slit, while the receiving slit was set at 0.2°. The signal from the counter for each step was sent to the computer where the intensity of each 0.02° 2θ step was recorded and the various X-ray corrections were applied. By summation, the integrated intensity of each X-ray peak determined the relative integrated intensities or texture coefficients for each peak calculated by

$$T_{c(hkl)} = \frac{I_{(hkl)}/I^0_{(hkl)}}{\frac{1}{N}\sum_{i=1}^{N} I_{(hkl)}/I^0_{(hkl)}} \quad (1)$$

where $I_{(hkl)}$ is the integrated intensity from an hkl peak, and $I^0_{(hkl)}$ is the integrated intensity from the same hkl peak obtained from a powder sample which had random texture. A FORTRAN program was written for a VAX 11/730 to control the experiment and is available from the authors. Using this program, the data for Table 1 was obtained using samples from the various deposition conditions.

3. Results and discussion

The relationship between current efficiency and current density is shown in Fig. 2 for the electrodeposition of niobium from the FLINAK system. At 725° C the efficiency increases substantially with increase in current density. At 750 and 775° C the increase is small and at 800° C the efficiency decreases as the current density is raised. Fig. 2 also shows that the efficiency decreases progressively with increasing temperature for constant current density. This result is attributed to an acceleration at high temperatures of the disproportionation reaction involving NbF_7^- and NbF to form Nb^{4+} and effectively reduces the concentration of NbF for reduction to metal. A similar argument was used by Senderoff [2] in his explanation of the

Table 1. Texture coefficients

Bath	*Temp. (° C)*	*Sample number*	*Current density ($mA\,cm^{-2}$)*	*h k l X-ray reflections*						*Efficiency*	*Hardness*
				110	*200*	*211*	*220*	*310*	*222*		
FLINAK + K_2NbF_7	725	36	20.0	3.0	0.5	9.3	0.9	0.4	10.0	82%	111
		37	42.0	0.6	0.1	3.5	0.1	0.0	10.0	105%	124
	750	34	20.0	10.0	0.0	0.6	1.9	0.1	0.0	79%	109
		40	21.0	10.0	0.0	6.1	1.9	4.1	0.0	82%	–
		41	22.0	10.0	0.0	0.3	2.2	0.0	0.0	84%	–
		42	22.0	10.0	0.0	0.6	1.7	0.0	0.8	75%	–
		43	22.0	10.0	0.0	2.8	1.7	0.1	0.3	82%	–
		44	24.0	10.0	0.0	2.5	1.8	0.1	0.0	83%	–
		35	40.0	10.0	0.0	2.6	1.9	0.0	1.2	88%	110
	775	24	15.0	10.0	0.0	1.8	1.8	0.9	0.0	78%	89
		26	18.0	10.0	0.0	0.6	2.4	0.4	0.0	80%	–
		28	20.0	10.0	0.0	0.3	1.9	0.3	0.0	76%	96
		30	30.0	10.0	0.5	3.9	1.9	4.9	0.0	76%	111
		31	40.0	10.0	0.0	1.4	2.3	1.7	0.4	86%	102
	800	33	20.0	10.0	0.0	5.7	2.3	2.3	0.0	73%	113
		32	50.0	10.0	0.0	1.6	2.3	0.5	0.0	66%	115
Binary + K_2NbF_7	750	56	8.5	0.7	10.0	2.4	0.3	8.8	0.0	63%	119
		63	16.6	1.3	0.0	10.0	0.4	0.1	3.8	60%	–
		64	16.6	2.3	0.0	10.0	0.7	0.2	3.1	64%	–
		52	24.0	2.9	9.4	3.9	0.6	10.0	0.1	77%	–
		57	25.5	4.0	0.0	10.0	1.2	0.6	8.7	79%	–
		58	33.7	1.5	0.0	10.0	0.0	0.9	0.0	77%	–
	775	61	9.7	2.2	10.0	1.2	0.4	4.0	0.0	70%	–
		60	19.4	7.3	9.3	1.3	1.8	10.0	0.0	70%	–
		65	22.7	8.7	0.3	10.0	1.7	1.1	1.6	71%	–
		66	28.8	10.0	0.0	5.9	2.5	0.3	0.5	72%	–
		67	34.4	7.5	0.4	10.0	1.4	1.1	2.2	73%	–
	800	71	10.5	10.0	0.0	2.5	1.7	0.2	0.1	50%	–
		70	20.4	10.0	0.0	1.7	2.0	0.2	3.0	62%	–
		72	26.3	10.0	0.0	1.6	2.2	0.1	0.0	70%	125
		76	26.7	10.0	0.0	0.8	2.8	0.1	0.0	67%	132
		62	27.8	10.0	0.1	3.2	2.7	4.1	0.0	78%	–
		69	34.4	10.0	0.0	0.3	2.2	0.0	0.0	76%	–
	875	77	12.5	10.0	1.0	4.7	2.0	6.2	0.0	51%	–
		78	21.7	10.0	0.1	8.8	1.9	7.9	0.0	68%	133
		79	25.0	10.0	0.0	9.8	2.2	9.8	0.3	82%	144

		80	30.0	5.3	0.0	4.7	1.3	10.0	0.0	80%	131
		75	35.7	6.6	1.2	9.8	0.9	10.0	0.0	74%	–
Binary mix + 5 wt % K_3CrF_4	800	97	8.0	10.0	0.1	7.1	1.5	0.9	0.6	–	–
		93	17.0	6.3	0.9	10.0	1.4	1.1	1.1	–	141
		91	30.0	9.4	0.0	10.0	2.6	0.4	4.6	63%	–
	850	99	20.0	6.6	0.0	10.0	1.6	0.3	0.8	54%	–
		98	21.0	7.5	0.0	10.0	1.8	0.3	2.5	58%	–
	875	100	20.0	8.8	0.1	10.0	1.8	0.4	0.5	61%	–
		101	20.0	10.0	0.0	9.5	2.7	0.0	1.2	–	145
		102	20.0	6.9	0.4	10.0	2.2	0.6	2.2	–	146
		90	22.0	10.0	0.0	1.6	2.5	0.0	0.0	54%	–
		92	32.0	8.9	0.1	10.0	2.7	0.5	1.6	61%	–
Binary mix + 10 wt % $NaBF_4$	750	108	15.0	0.0	0.0	0.0	0.0	0.0	0.0	–	–
		107	23.0	0.5	10.0	0.0	0.0	1.5	0.0	32%	213
		126	32.0	6.1	10.0	1.7	1.3	5.4	0.0	75%	–
		127	39.0	3.4	10.0	1.3	0.8	5.0	0.0	70%	–
		128	55.0	1.5	10.0	0.5	0.1	2.5	0.0	97%	–
		129	75.0	0.4	10.0	0.6	0.0	1.0	0.0	86%	–
		130	83.0	0.3	10.0	0.4	0.0	0.3	0.0	84%	–
	850	111	25.0	2.5	10.0	2.2	0.6	5.3	0.0	34%	157
		120	30.0	4.3	10.0	5.5	1.9	9.0	0.3	89%	158
		121	32.0	2.7	10.0	2.8	0.7	6.0	0.1	85%	142
		113	34.0	3.8	10.0	2.5	1.0	2.2	0.1	78%	107
FLINAK + K_2NbF_7 + K_2TaF_7	775	138*	17.0	10.0	0.0	5.9	2.4	0.3	0.6	50%	–
		139*	22.0	1.9	0.1	10.0	0.3	0.0	1.2	76%	–
		140*	31.0	3.6	0.7	10.0	0.9	0.2	3.6	80%	–
		145†	18.0	0.0	10.0	0.0	0.0	1.6	0.0	50%	–
		142†	22.0	0.0	10.0	0.0	0.0	0.0	0.0	71%	–
		143†	23.0	0.0	10.0	0.0	0.0	0.0	0.0	74%	–
		144†	26.0	0.0	10.0	0.0	0.0	0.4	0.0	75%	–
		148‡	15.0	0.0	10.0	0.0	0.0	2.3	0.0	62%	–
		147‡	23.0	0.0	10.0	0.0	0.0	0.8	0.0	67%	–
		151‡	29.0	1.9	10.0	0.4	0.3	8.7	0.0	79%	–
		149‡	32.0	0.0	10.0	0.0	0.0	0.5	0.0	82%	–
		150‡	37.0	0.1	10.0	0.0	0.0	0.8	0.0	86%	–
		157§	16.0	0.4	10.0	0.1	0.0	4.8	0.0	78%	–
		154§	24.0	0.0	10.0	0.0	0.0	0.7	0.0	75%	–
		153§	30.0	0.0	10.0	0.0	0.0	0.0	0.0	70%	–
		155§	30.0	0.0	10.0	0.0	0.0	1.2	0.0	82%	–
		156§	33.0	1.2	10.0	0.1	0.1	4.7	0.0	83%	–

Concentrations of K_2TaF_7: * 2 wt %; † 50 wt %; ‡ 7.5 wt %; § 10 wt %. Note: 12.5 wt % K_2TaF_7 bath results omitted from table.

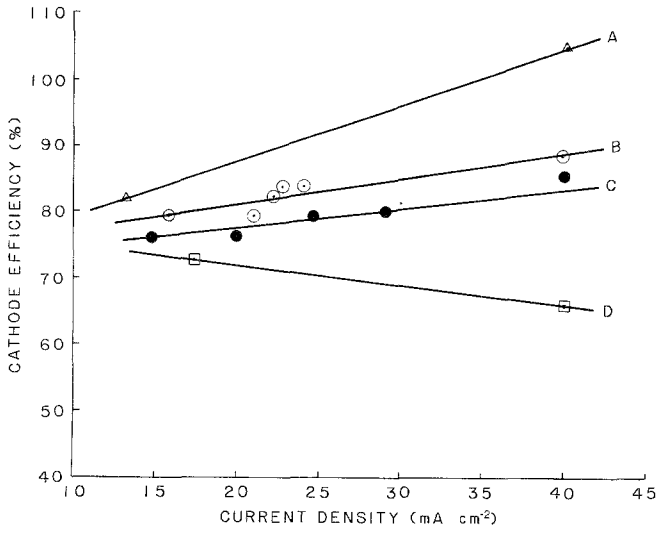

Fig. 2. Variation of cathode efficiency with current density for the electrodeposition of niobium from LiF–NaF–KF + K_2NbF_7 at 725° C (A), 750° C (B), 775° C (C) and 800° C (D). Efficiency based on a four-electron change in oxidation state.

observed decrease in efficiency at low current densities for the FLINAK system.

By comparison, the variation of efficiency for the binary eutectic (Fig. 3) is more complex. For all temperatures concerned, the efficiency was seen to increase with current density, to pass through a maximum between 25 and 30 mA cm^{-2}, and then to drop off at higher current densities. While the origin of the maximum is uncertain, a trend was established relating the plating efficiencies to the ratio of anode weight loss to cathode weight gain (A/C). The spread of A/C varied from near unity to 2.5. Higher efficiencies were associated with A/C values approaching unity and lower efficiencies associated with A/C values approaching 2.5. The significance of a high A/C ratio is that a larger number of NbF_7^- ions are present during the electrodissolution of the anode and, consequently, the formation of niobium metal at the cathode is restricted once more by an enhancement of the disproportionation reaction.

The grain size of niobium deposits prepared from both types of electrolytes is influenced by current density. Fig. 4 illustrates that some grain refinement was obtained by increasing the current density from 10 to 40 mA cm^{-2} in the plating of niobium from FLINAK. Fig. 5 shows a similar trend in grain refinement for the plating of niobium from NaF–KF. However, the slight refinement in grain size is not reflected in deposit hardness. In general, hardness values for deposits associated with FLINAK vary between 102 and 124 KHN (Knoop hardness number), while deposits produced from KF–NaF vary between 119 and 144 KHN.

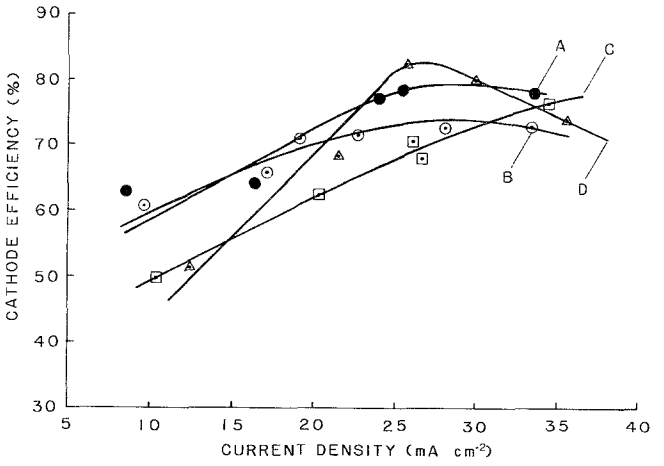

Fig. 3. Variation of cathode efficiency with current density for the electrodeposition of niobium from KF–NaF + K_2NbF_7 at 750° C (A), 775° C (B), 800° C (C) and 875° C (D). Efficiency based on a four-electron change in oxidation state.

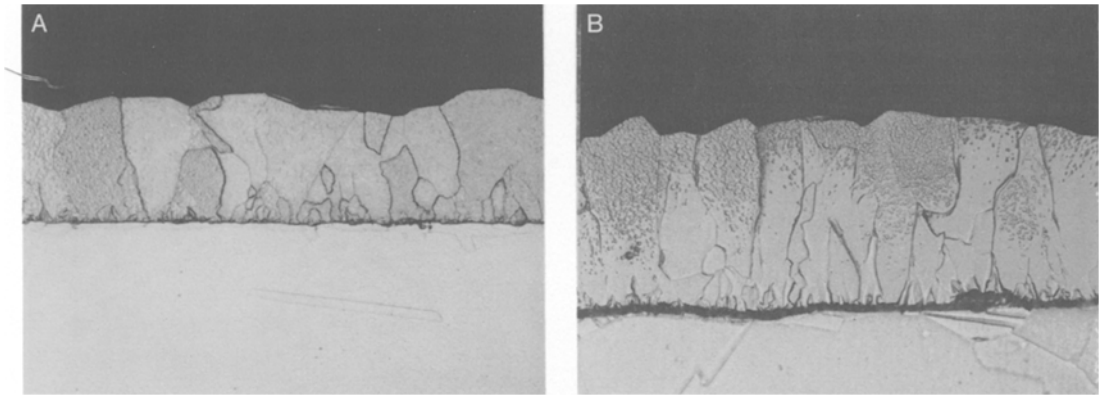

Fig. 4. Microstructure of niobium plated at 775° C from LiF–NaF–KF + K_2NbF_7. (A) 10 mA cm^{-2}; (B) 40 mA cm^{-2}. × 120.

The introduction of cationic additions to molten salt electrolytes produced interesting changes in deposit morphology and orientation. Tantalum added as K_2TaF_7 in the range of 5 to 10 wt % produced bright niobium deposits from the FLINAK bath. Above and below this concentration the deposit structure and surface features appear similar to those plated without tantalum additions. It is interesting to note that these changes occur in the absence of tantalum codeposition. In all cases, analyses using an electron microprobe verified the absence of tantalum in the deposits. Sample 153 of Table 1 is a typical bright deposit plated from a FLINAK electrolyte containing 10 wt % K_2TaF_7. Its surface texture can be seen in Fig. 6D and its microstructure consisting of fine columnar grains is seen in Fig. 7. These features may be compared with deposits prepared without tantalum addition in Figs 4 (sample 26) and 6A. It was observed that bright deposits were obtained only in samples showing pure [1 0 0] orientation, i.e. sample numbers 142, 143 and 153. Brightness in the deposits gradually diminished with the appearance of mixed orientation. The orientation in deposits prepared without tantalum additions was notably different. At 725° C the deposits started with a [2 1 1] texture and as the current density increased from 18 to 42 mA, the texture changed to [1 1 1]. When the bath was increased to 750° C the texture of the deposit became predominantly [1 1 0] and remained so as the temperature was increased to 775° C. As the bath reached 800° C, the deposit was almost random at low current densities and some [1 1 0] texture developed as the current density was increased to 50 mA.

The addition of K_3CrF_6 up to 5 wt % pro-

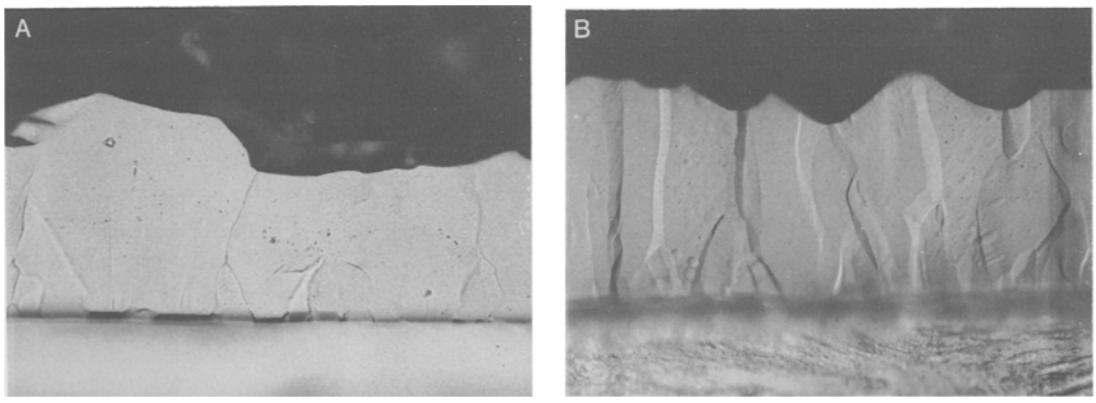

Fig. 5. Microstructure of niobium plated at 750° C from NaF–KF + K_2NbF_7. (A) 8.5 mA cm^{-2}; (B) 33.7 mA cm^{-2}. × 300.

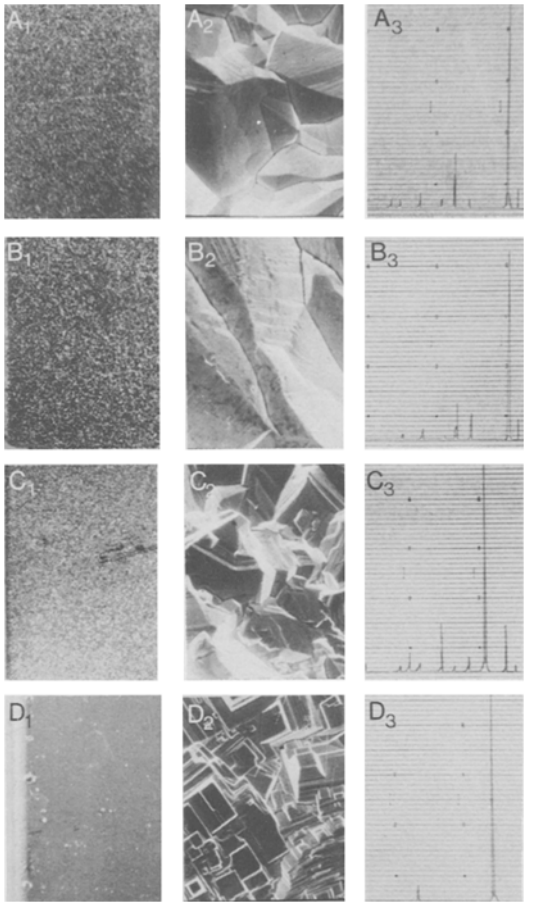

Fig. 6. Surface view (subscript 1) and SEM of niobium surface (subscript 2) and X-ray reflections (subscript 3). (A), LiF–NaF–KF + K_2NbF_7; (B), NaF–KF + K_2NbF_7; (C), NaF–KF + K_2NbF_7 + 10 wt % $NaBF_4$; (D), LiF–NaF–KF + K_2NbF_7 + 10 wt % K_2TaF_7. Surface view, × 20; SEM, × 1000.

duced no observable differences in the morphology, orientation or physical properties of niobium deposits produced from the NaF–KF bath. However, the addition of 10 wt % $NaBF_4$ (sample number 126) markedly altered the growth orientation, surface texture (Fig. 6C) and microstructure (Fig. 8). While the presence of boron in the niobium deposits was verified, quantitative evaluations were not made. Fig. 6B and 6C shows a comparison of the surface features of niobium deposits plated with and in the absence of boron addition.

The formation of deposit texture is dependent on boron incorporation as well. In this case a [1 1 0] texture is predominant and, depending

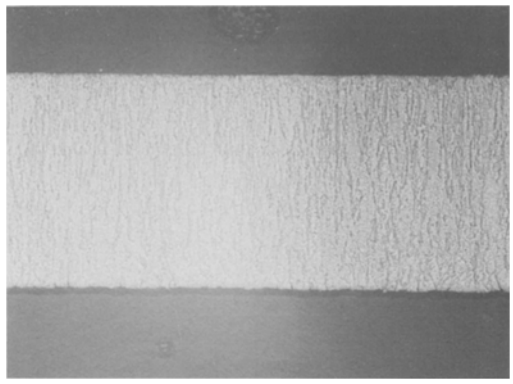

Fig. 7. Microstructure of niobium plated at 775° C from LiF–NaF–KF + K_2NbF_7 + 10 wt % K_2TaF_7. × 120.

upon the temperature and current density, some [3 1 0] orientation emerges from the formation of a duplex texture. In the absence of boron additions, the binary bath cannot be adequately characterized by a single texture. At the lower temperature of 750° C the [2 1 1] texture is predominant. At 775° C no dominant trend in the formation of texture is observed. At 800° C a combination of samples with [1 1 0] and random orientation is obtained. At 875° C a [3 1 0] orientation becomes mixed with a [2 1 1] orientation to form a duplex type texture.

4. Conclusion

Observations have been made on the effects of temperature, current density, and additions of K_3CrF_4 and K_2TaF_7 on the structure and efficiency of the niobium deposits. Maxima were

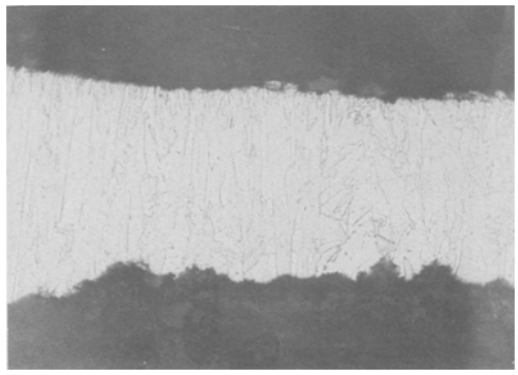

Fig. 8. Microstructure of niobium plated at 750° C from NaF–KF + K_2NbF_7 + 10 wt % $NaBF_4$. × 120.

found in the plots of current efficiency versus current density for the KF–NaF solvent system, while linear relationships were obtained for FLINAK. The effect of various additives resulted in improvements in surface finish, grain size and hardness. Although some correlation was observed between the texture and other properties studied, no attempt was made to study the growth mechanisms during electrocrystallization. Finally, it has been shown that the addition of tantalum and boron to the electrolyte produced deposits with improved properties.

Acknowledgements

The authors are greatly indebted to the support work provided by Chris Rickard and Leo McNamara who were invaluable for their aid and expertise in the fields of metallography and scanning electron microscopy.

References

[1] S. Senderoff and G. W. Mellors, *Science* **153** (1966) 1495.
[2] S. Senderoff, *Metall. Revs.* **11** (1966) 97.
[3] D. Inman and S. H. White, Proceedings of the International Symposium on Molten Salt Electrolysis in Metal Production, Grenoble, IMM (1977) pp. 51–61.
[4] D. Inman, Proceedings of the European Conference on Development of Molten Salts Applications, Geneva, Battelle (1973) pp. 58–61.
[5] G. W. Mellors and S. Senderoff, *J. Electrochem. Soc.* **112** (1965) 266.
[6] *Idem*, *Plating* **51** (1964) 972.
[7] C. Decroly, A. Mukhtar and R. Winand, *J. Electrochem. Soc.* **115** (1968) 905.
[8] V. Cohen, *J. Electrochem. Soc.* **128** (1981) 731.
[9] T. Yoko and R. A. Bailey, Proceedings of the First International Symposium on Molten Salt Chemistry and Technology, Kyoto, Japan (1983) pp. 111–14.